THE TALENTED MR. INVERSIVE TRIANGLE IN THE ELLIPTIC BILLIARD

DAN REZNIK, RONALDO GARCIA, AND MARK HELMAN

ABSTRACT. Inverting the vertices of elliptic billiard N-periodics with respect to a circle centered on one focus yields a new "focus-inversive" family inscribed in Pascal's Limaçon. The following are some of its surprising invariants: (i) perimeter, (ii) sum of cosines, and (iii) sum of distances from inversion center (the focus) to vertices. We prove these for the N=3 case, showing that this family (a) has a stationary Gergonne point, (b) is a 3-periodic family of a second, rigidly moving elliptic billiard, and (c) the loci of incenter, barycenter, circumcenter, orthocenter, nine-point center, and a great many other triangle centers are circles.

Keywords invariant, elliptic, billiard, inversion.

 \mathbf{MSC} 51M04 and 51N20 and 51N35 and 68T20

1. Introduction

In [15] we introduced the "focus-inversive" polygon, whose vertices are inversions of elliptic billiard N-periodic vertices with respect to a circle centered on one focus. Since N-periodics are inscribed in an ellipse, the focus-inversive family will be inscribed in Pascal's Limaçon [4]; see Figure 1.

A classic invariant of billiard N-periodics is perimeter [20]. Recently, the sum of cosines was proved as an interesting derived invariant [1, 2]. Surprisingly, and still pending proof, for all N, the focus-inversive family also conserves perimeter and sum-of-cosines! Additionally, and as a corollary to the invariant sum-of-cosines, the sum of distances from the focus to inversive vertices is invariant [16].

For generic Poncelet families, the loci of vertex and area centroids are conic though in general the *perimeter* centroid is not [18, Thm 1]. Interestingly, the loci of the 3 aforementioned centroids over the focus-inversive family in the elliptic billiard are numerically circles for all N, also unproven.

Main contributions: In this article we concentrate on properties of the focus-inversive family derived from elliptic billiard 3-periodics:

- In Section 3: The perimeter and sum of cosines are invariant, and the family is a billiard family to a rigidly-moving ellipse, whose center moves along a circle; the Gergonne point [21] of the family is stationary.
- Section 4: The sum of distances from the inversion center (a focus) to each vertex is invariant as is the product of areas of left- and right-focus-inversive triangles.

Date: November 2020.

¹Any "new" invariants are dependent upon the two integrals of motion – linear and angular momentum – that render the elliptic billiard an integrable dynamical system [9].

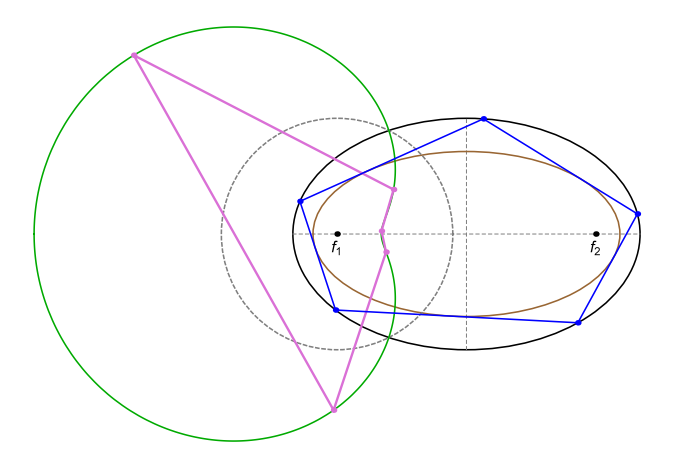


FIGURE 1. For a generic N-periodic (blue, N=5) with vertices P_i , the inversive polygon (pink) is inscribed in Pascal's Limaçon (green) and has vertices at inversions of the P_i with respect to a circle (dashed black) centered on f_1 . For all N, the focus-inversive perimeter, sum of cosines[‡], and sum of focus-to-vertex distances are experimentally invariant [15]. [‡] Sum of focus-inversive cosines is variable for N=4 simple and a certain self-intersected N=6 [6]. Video.

• Section 5: the loci of 29 of the first 100 centers listed in [10] are *circles*, and these include the vertex, area, and perimeter centroids. "Why so many circles?" is a fair and unanswered question.

Regarding the last result, we further observe that (i) centers whose loci are ellipses over the original 3-periodics become circles in the focus-inversive case, except for X_k , k = 88, 162, in the $k \le 200$ range; (ii) some centers of the original 3-periodics whose loci are non-elliptic produce elliptic loci over the focus-inversive family. Examples include: X_k , k = 69, 75, 85, 86 in the $k \le 100$ range.

In Appendix A we review some classical quantities of the elliptic billiard. In Appendix B we provide explicit expressions for vertices and caustics of 3-periodics. A reference table with all symbols used appears in Appendix C. A link to a YouTube animation is provided in the caption of most figures. Table 1 in Section 6 compiles all videos mentioned.

Related Work. Experimentation with the dynamic geometry of 3-periodics in the elliptic billiard evinced that the loci of the incenter, barycenter, and circumcenter are ellipses. These observations were soon proved [5, 17, 18]. Indeed, using a combination of numerical and computer-algebra methods, we showed that the loci of a full 29 out of the first 100 centers listed in Kimberling's Encyclopedia [10] are ellipses [7].

2. Preliminaries

Throughout this article we assume the elliptic billiard is the ellipse:

(1)
$$f(x,y) = \left(\frac{x}{a}\right)^2 + \left(\frac{y}{b}\right)^2 = 1, \quad a > b > 0.$$

Let $\delta = \sqrt{a^4 - a^2b^2 - b^4}$ and ρ denote the radius of the inversion circle. The eccentricity $\varepsilon = \sqrt{1 - (b/a)^2}$, and $c^2 = a^2 - b^2$.

A word about our proof method. We omit most proofs as they have been produced by a consistent process, namely: (i) using Appendix B to obtain symbolic expressions for the vertices of an isosceles 3-periodic, i.e., whose first vertex $P_1 = (a,0)$; (ii) obtain a symbolic expression for the invariant of interest, (iii) simplify it (both human intervention and CAS), and finally (iv) verify its validity symbolically and/or numerically over several N-periodic configurations and elliptic billiard aspect ratios a/b.

3. Focus-Inversives and the Rotating Billiard Table

A generic N>3 focus-inversive polygon is illustrated in Figure 1. This is a polygon whose vertices are inversions of the N-periodic vertices wrt a circle of radius ρ centered on focus f_1 .

It is well known the inversion of an ellipse w.r.t. a focus-centered unit circle is Pascal's Limaçon $\mathcal{L}(t)$ [4], given by:

$$\mathcal{L}(t) = \left[-a\cos t(\varepsilon\cos t + 1) - c, a\sin t(\varepsilon\cos t + 1) \right], \quad 0 \le t \le 2\pi$$

Therefore:

Remark 1. For any N, the focus-inversive family is inscribed in $\mathcal{L}(t)$.

As shown in Figure 3 is the non-conic caustic to the N=3 focus-inversive family. As a/b is increased, the caustic transitions from (i) a regular curve, to (ii) one with a self-intersection and two cusps, to (iii) a non-compact curve with two infinite branches.

Figure 2 illustrates the N=3 focus-inversive triangle. Recall two well-known triangle centers: the Gergonne point X_7 is the perspector of the incircle and the Mittenpunkt X_9 is the point of concurrence of lines drawn from the excenters through the side midpoints [10].

Proposition 1. Over the 3-periodic family, the Gergonne point X_7^{\dagger} of focus-inversive triangles is stationary on the billiard's major axis at location:

$$X_7^{\dagger} = \left[c \left(1 - \frac{\rho^2}{\delta + c^2} \right), 0 \right]$$

Note: let X_7^{\ddagger} denote the inversion of X_7^{\dagger} with respect to the same inversion circle used above. Then:

$$X_7^{\ddagger} = \left[\frac{\delta}{c}, 0\right]$$

Proposition 2. Over the 3-periodic family, the Mittenpunkt X_9^{\dagger} of focus-inversive triangles moves along a circle with center and radius given by:

$$C_9^{\dagger} = \left[-c \left(1 + \rho^2 \frac{1}{2b^2} \right), 0 \right]$$

$$R_9^{\dagger} = \rho^2 \frac{2a^2 - b^2 - \delta}{2ab^2}$$

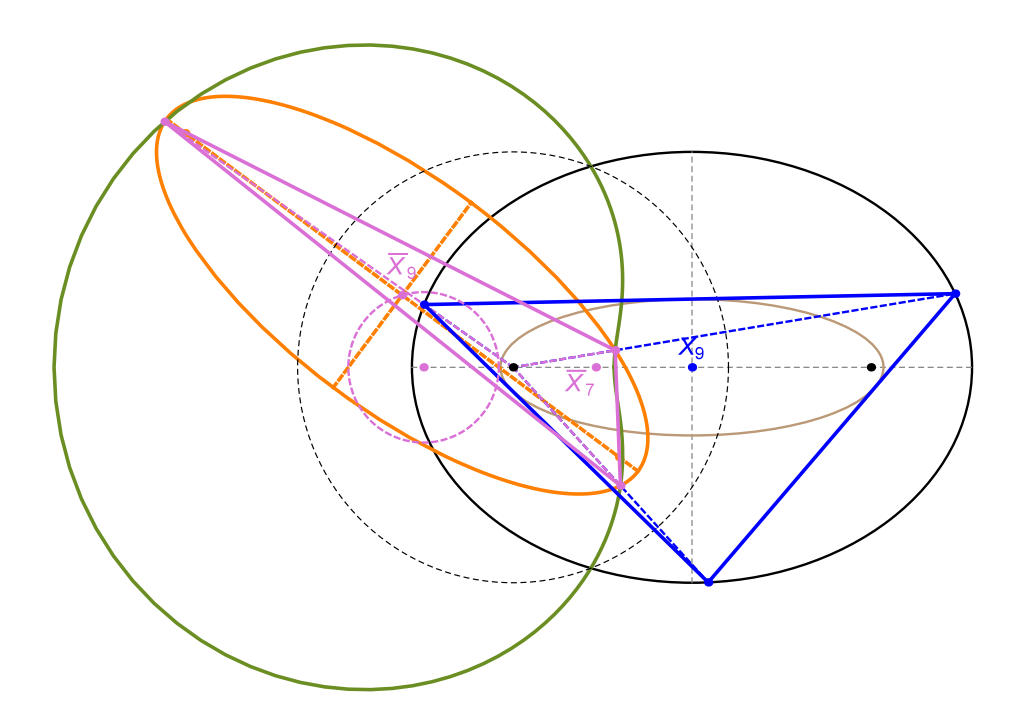


FIGURE 2. The vertices of 3-periodics (blue), when inverted with respect to a unit circle (dashed black) centered on a focus, produce a family of constant perimeter triangles (pink). Their X_9 -centered circumellipses (orange) rigidly translate and rotate (invariant semi-axes) with their center (\bar{X}_9) moving along a circle. The Gergonne point \bar{X}_7 of the inversive family is stationary. Video 1, Video 2

Note: let C_9^{\ddagger} denote the inversion of C_9^{\dagger} with respect to the same inversion circle used above. Then:

$$C_9^{\ddagger} = \left[-\frac{a^2 + b^2}{c}, 0 \right]$$

Proposition 3. The X_9 -centered circumellipse C^{\dagger} of the N=3 inversive family has invariant semi-axes a^{\dagger} and b^{\dagger} given by:

$$a^{\dagger} = \rho \, k_1 \sqrt{k_2 \, (\delta + a \, c)}$$

$$b^{\dagger} = \rho \, k_1 \sqrt{k_2 \, (\delta - a \, c)}$$
where:
$$k_1 = \frac{c\sqrt{2}}{k_3} \sqrt{(8 \, a^4 + 4 \, a^2 b^2 + 2 \, b^4) \, \delta + 8 \, a^6 + 3 \, a^2 b^4 + 2 \, b^6}$$

$$k_2 = 2a^2 - b^2 - \delta$$

$$k_3 = 2ab^2 \, \left(\left(2 \, a^2 - b^2 \right) \, \delta + 2 \, a^4 - 2 \, a^2 b^2 - b^4 \right)$$

Note: C^{\dagger} is the rigidly-moving circumbilliard [12] of the inversive polygon.

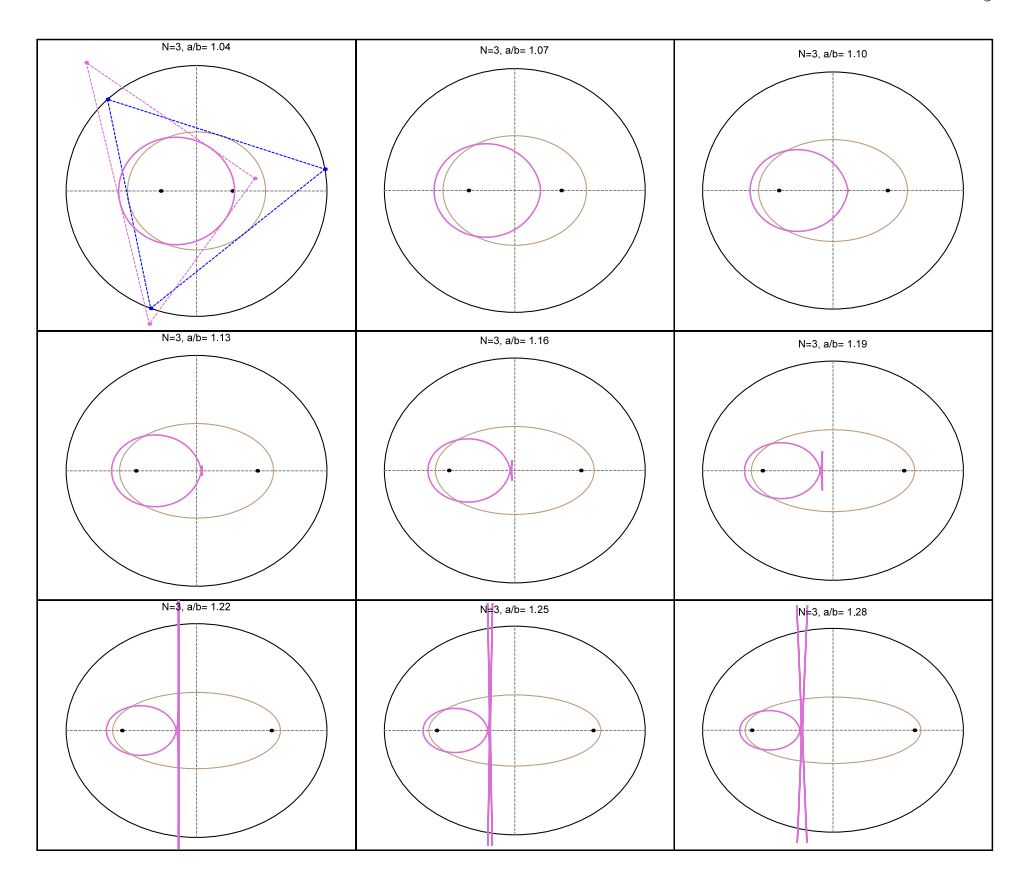


FIGURE 3. Non-conic caustic (pink) to the focus-inversive family (pink). As a/b increases, said caustic transitions from (i) regular, to (ii) a curve with one self-intersection and two cusps, to (iii) a non-compact curve. A sample 3-periodic (dashed blue) and the corresponding focus-inversive triangle (dashed pink) is shown on the first frame only. The billiard confocal caustic (brown) is shown on every frame. App

Proposition 4. The perimeter L^{\dagger} of the N=3 focus-inversive family is invariant and given by:

$$L^{\dagger} = \rho^2 \frac{\sqrt{(8 a^4 + 4 a^2 b^2 + 2 b^4) \delta + 8 a^6 + 3 a^2 b^4 + 2 b^6}}{a^2 b^2}$$

In turn, the above entail:

Theorem 1. With respect to a reference system centered on \bar{X}_9 and oriented along the semi-axes of C^{\dagger} , the inversive N=3 family is a 3-periodic billiard family of C^{\dagger} .

Experimentally we have observed:

Conjecture 1. The perimeter of the focus-inversive polygon is invariant for any N.

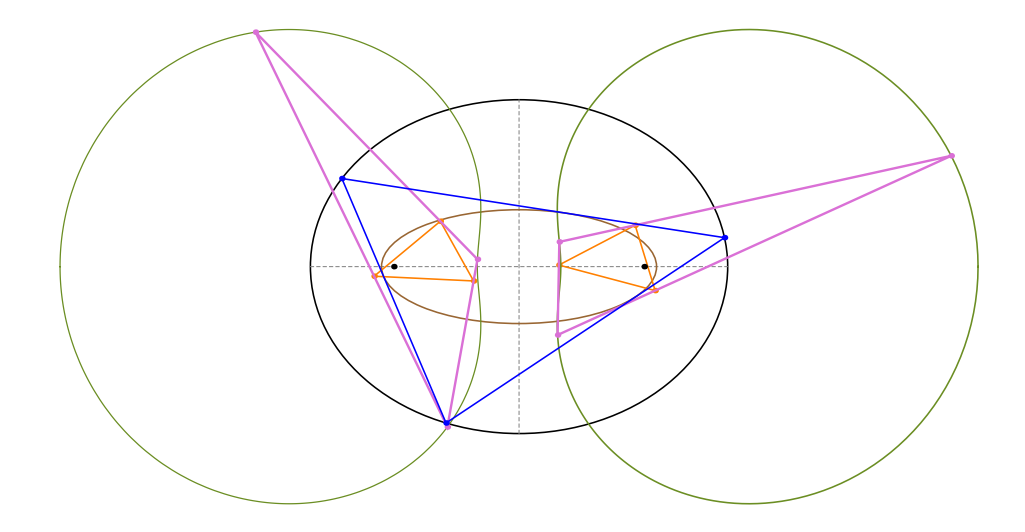


FIGURE 4. f_1 - and f_2 -inversive triangles are shown (pink). The product of their areas is invariant. Also shown are the f_1 - and f_2 -pedal polygons (orange) to said triangles. Their areas are variable but dynamically equal. Video

4. More Focus-Inversive Invariants

Proposition 5. For N=3, the sum of focus-inverse spoke lengths $\sum 1/d_{1,i}$ is invariant and given by:

$$\sum 1/d_{1,i} = \frac{a^2+b^2+\delta}{ab^2}$$

Proposition 6. For N=3, the sum of focus-inversive cosines $\sum \cos \theta_{1,i}^{\dagger}$ is given by:

$$\sum \cos \theta_{1,i}^{\dagger} = \frac{\delta(a^2 + c^2 - \delta)}{a^2 c^2}$$

Referring to Figure 4:

Proposition 7. For N=3, the area product $A_1^{\dagger}.A_2^{\dagger}$ of the two focus-inversive triangles is given by:

$$A_1^{\dagger}.A_2^{\dagger} = \frac{\rho^8}{8a^8b^2} \left[\left(a^4 + 2 a^2b^2 + 4 b^4 \right) \delta + a^6 + (3/2) a^4b^2 + 4 b^6 \right]$$

Observation 1. The areas of both pedal triangles of the focus-inversives with respect to the respective foci are dynamically equal.

5. CIRCULAR LOCI OF TRIANGLE CENTERS

In [7] we showed that amongst the first 100 triangle centers listed on [10], the following 29 sweep an elliptic locus over 3-periodics in the elliptic billiard: X_k , k=1, 2, 3, 4, 5, 7, 8, 10, 11, 12, 20, 21, 35, 36, 40, 46, 55, 56, 57, 63, 65, 73, 78, 79, 80, 84, 88, 90, 100. Notably, the Mittenpunkt X_9 is stationary at the billiard center [14]. Referring to Figure 5:

Theorem 2. Amongst the first 100 triangle centers listed on [10], the following 28 sweep a circular locus over focus-inversive 3-periodics in the elliptic billiard: X_k^{\dagger} , k=1, 2, 3, 4, 5, 8, 9, 10, 11, 12, 20, 21, 35, 36, 40, 46, 55, 56, 57, 63, 65, 73, 78, 79, 80, 84, 90, 100. All centers lie on the billiard major axis.

Proof. Symbolic manipulation and numeric verification.

Through painstaking CAS-assisted simplification, we were able to obtain compact expressions for only a few of the above circular loci, namely: X_k , k = 1, 2, 3, 4, 5, 9, 11, 100.

Proposition 8. The locus of X_1^{\dagger} is the circle given by:

$$\begin{split} C_1^{\dagger} &= \left[c \left(-1 + \rho^2 \frac{-2a^2 + b^2 + 2\delta}{2b^4} \right), 0 \right] \\ R_1^{\dagger} &= \rho^2 \frac{-2\delta^2 + b^4 + (2a^2 - b^2)\delta}{2ab^4} \end{split}$$

Proposition 9. The locus of X_2^{\dagger} is the circle given by:

$$C_2^{\dagger} = \left[-c \left(1 + \rho^2 \frac{2a^2 - b^2 - \delta}{3a^2b^2} \right), 0 \right]$$

$$R_2^{\dagger} = \rho^2 \frac{2a^2 - b^2 - \delta}{3ab^2}$$

Proposition 10. The locus of X_3^{\dagger} is the circle given by:

$$C_3^{\dagger} = \left[-c \left(1 + \rho^2 \frac{a^2 + b^2}{2b^4} \right), 0 \right]$$

$$R_3^{\dagger} = \rho^2 \frac{a(-b^2 + \delta)}{2b^4}$$

Proposition 11. The locus of X_4^{\dagger} is the circle given by:

$$C_4^{\dagger} = \left[c \left(-1 + \rho^2 \frac{(b^2 + \delta)\delta}{a^2 b^4} \right), 0 \right]$$

$$R_4^{\dagger} = \rho^2 \frac{c^2 (b^2 + \delta)}{a b^4}$$

Proposition 12. The locus of X_5^{\dagger} is the circle given by:

$$\begin{split} C_5^{\dagger} &= \left[c \left(-1 + \rho^2 \frac{a^4 - 3a^2b^2 + 2b^4 + 2b^2\delta}{4a^2b^4} \right), 0 \right] \\ R_5^{\dagger} &= \rho^2 \frac{(3a^2 - 2b^2)b^2 + (a^2 - 2b^2)\delta}{4ab^2} \end{split}$$

Proposition 13. The locus of X_{11}^{\dagger} is the circle given by:

$$\begin{split} C_{11}^{\dagger} &= \left[c \left(-1 + \rho^2 \frac{-a^2 + b^2 + \delta}{2a^2b^2} \right), 0 \right] \\ R_{11}^{\dagger} &= \rho^2 \frac{-a^2 + b^2 + \delta}{2ab^2} \end{split}$$

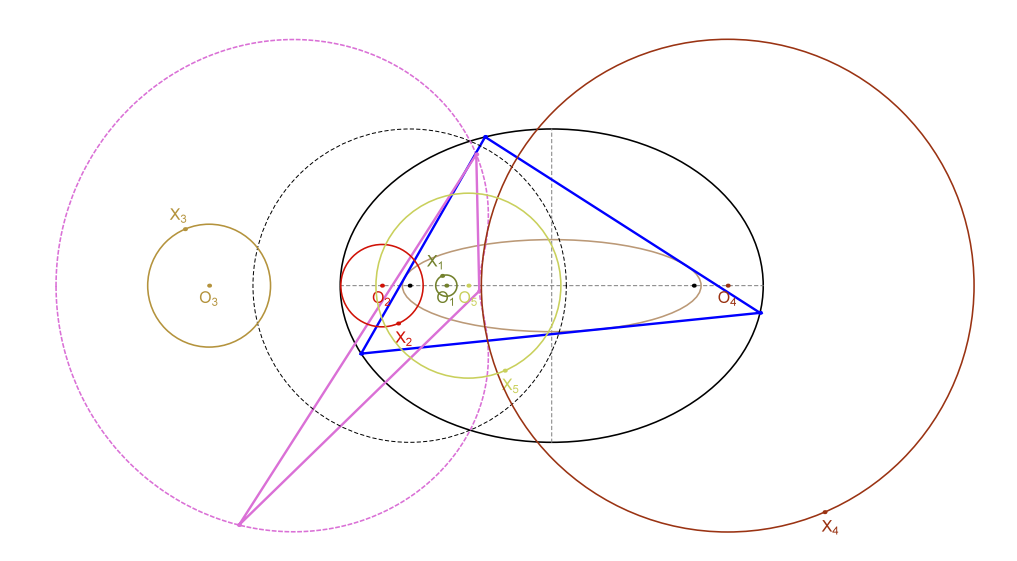


FIGURE 5. The focus-inversive 3-periodic (pink) is shown inscribed in Pascal's Limaçon (dashed pink). Also shown are the circular loci of X_k^{\dagger} , k=1,2,3,4,5. Notice all its centers O_i lie on the billiard's major axis. Video

Proposition 14. The locus of X_{100}^{\dagger} is the circle given by:

$$\begin{split} C_{100}^{\dagger} &= \left[-c\left(1+\rho^2\frac{1}{b^2}\right), 0\right] \\ R_{100}^{\dagger} &= \rho^2\frac{a}{b^2} \end{split}$$

As noted above, the focus-inversive Gergonne point X_7^\dagger is stationary on the major axis.

In [13] triangle centers whose locus over 3-periodics was the billiard boundary were called "swans". As it was shown, both X_{88} and X_{100} are swans [13]. Curiously, the former's (resp. latter's) motion is non-monotonic (monotonic) with respect to a continuous clockwise parametrization of 3-periodics.

Referring to Figure 7:

Observation 2. Amongst all 29 triangle centers whose locus is an ellipse over 3-periodics, only X_{88}^{\dagger} does not sweep a circular locus over the focus-inversive family. Nevertheless, this locus is algebraic, regular, can be both convex and concave, and is symmetric wrt major axis of the ellipse.

Referring to Figure 6, X_{162} is yet another example of a billiard "swan" whose focus-inversive locus is non-elliptic.

Observation 3. For $101 \le k \le 1000$, the following 68 focus-inversive triangle centers also sweep circular loci: X_k^{\dagger} , k = 104, 119, 140, 142, 144, 145, 149, 150, 153, 165, 191, 200, 210, 214, 224, 226, 329, 354, 355, 376, 377, 381, 382, 388, 390, 392, 404, 405, 411, 442, 443, 452, 474, 480, 484, 495, 496, 497, 498, 499, 546, 547, 548, 549, 550, 551, 553, 631, 632, 908, 920, 934, 936, 938, 942, 943, 944, 946, 950, 954, 956, 958, 960, 962, 993, 997, 999, 1000.

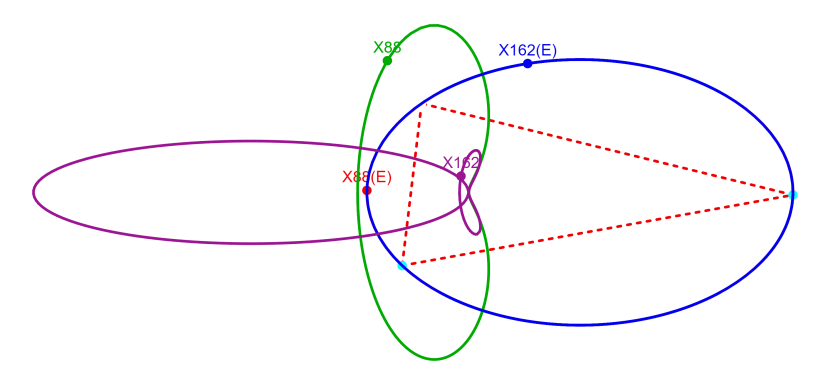


FIGURE 6. Over billiard 3-periodics (dashed red) the loci of both X_{88} and X_{162} coincide with the billiard (blue). However, when taken as centers of the the focus-inversive triangles (not shown), their loci are clearly non-elliptic (green and purple). Live app: $X_{88}+X_{162}$, $X_{88}+X_{100}$

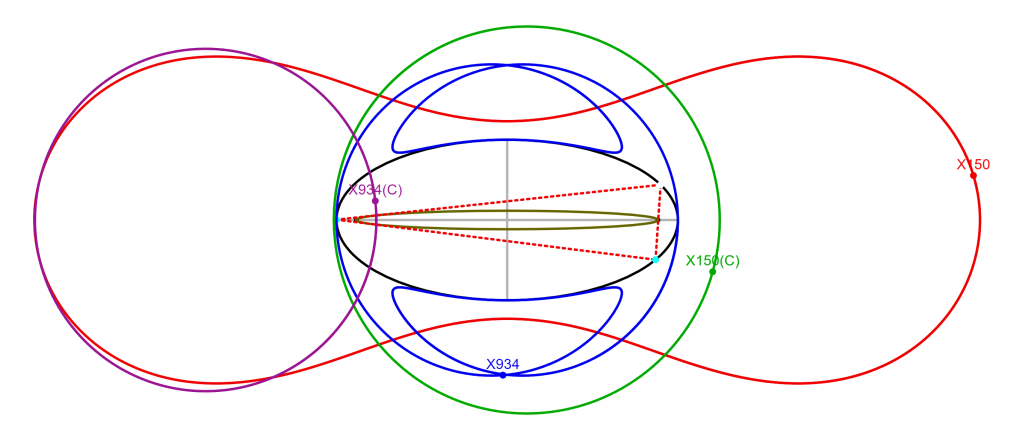


FIGURE 7. The locus of X_{150} is a dumbbell curve (red). Curiously, the locus of X_{150} over the focus inversives is a circle (green). Similarly, the billiard locus of X_{934} (blue) is a curve with two self-intersections; its locus over the focus-inversives is a circle (purple). App

Referring to Figure 7:

Observation 4. In the k=1,...,1000 range, the only triangle centers whose billiard locus is not an ellipse and whose focus-inversive locus is a circle are X_{150} and X_{934} . In fact, the latter's locus is identical to X_{100}^{\dagger} .

Observation 5. Over k = 1, ..., 1000, if the locus of X_k is an ellipse for billiard 3-periodics which is not the billiard itself, then the locus of X_k^{\dagger} over the focusinversives is a circle.

5.1. Locus of Perimeter Centroid. Let C_0 , C_1 , C_2 denote the vertex, perimeter, and area centroids of polygon, respectively. In [18, Thm 1] it was shown that the loci of C_0 , C_2 over Poncelet families are ellipses, though this not hold in general for C_1 .

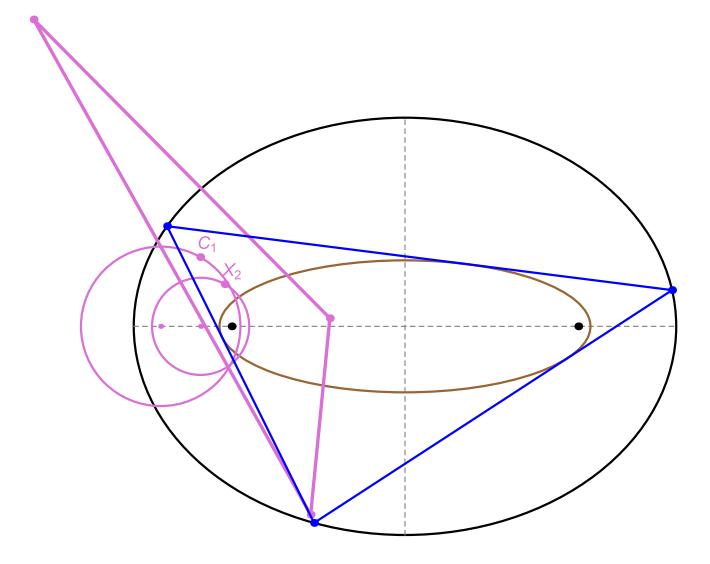


FIGURE 8. Circular locus of the focus-inversive X_2 and the perimeter centroid $C_1^{\dagger} = X_{10}^{\dagger}$. Note that for triangles, the former coincides with both the vertex and area centroids. App

For triangles, $C_0 = C_2 = X_2$ and $C_1 = X_{10}$ [21, Spieker Center]. Per above we already know that the locis of X_2 and X_{10} over the focus-inversive family are circles. Therefore, and referring to Figure 8:

Corollary 1. The loci of the C_i^{\dagger} , i=1,2,3 of the focus-inversive family are circles.

5.2. The Center-Inversive Triangle. Let the center-inversive triangle have vertices at the inversions of the P_i w.r.t. unit-radius circle concentric with the elliptic billiard; see Figure 9. Therefore this family is inscribed in Booth's curve (the inverse of an ellipse with respect to a concentric circle) [3]. As shown in Figure 10, as a/b increases, the caustic transitions from a convex-regular curve, to one with two self-intersections and cusps, to a non-compact one.

Proposition 15. The locus of the circumcenter X_3^{\odot} of the center-inversive triangle is an ellipse concentric, axis-aligned, and homothetic to the elliptic locus of X_3 of the billiard 3-periodics, at ratio $1/\delta$. Moreover, the aspect ratio of the locus of X_3^{\odot} is the reciprocal of that of the caustic.

Proof. The circumcircle of the center-inversive triangle is the inversion of the circumcircle of the billiard's 3-periodic. Denote by R and X_3 the circumradius and circumcenter of the 3-periodic, and by X_3^{\odot} the circumcenter of the center-inversive triangle. By properties of circle inversion, we have that the center of the billiard O, X_3 , and X_3^{\odot} are collinear, with $OX_3^{\odot} = \frac{OX_3}{OX_3^2 - R^2}$ (recall that the inversion of the center of a circle does not coincide with the center of the inverted circle). The quantity $OX_3^2 - R^2$ represents the power of point O with respect to the circumcircle of the 3-periodic. In [8, Thm 3], it was shown that the power of the billiard center with respect to this circumcircle is constant over the family of 3-periodics and equal to $-\delta$. Moreover, in [5] it was proved that the locus of X_3 is an ellipse axis-aligned

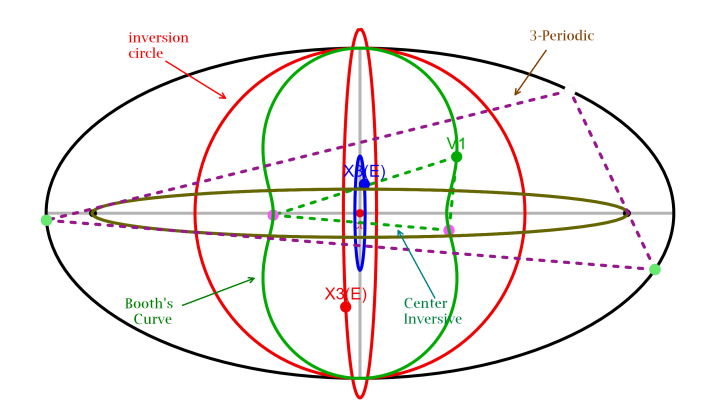


FIGURE 9. The center-inversive triangle (green) has vertices at the inversions of the 3-periodic vertices wrt unit-circle (red) concentric with the ellipse. It is inscribed in Booth's curve (green) [3]. Over the 3-periodics, the locus of X_3 is an ellipse (red) [5]. The locus of X_3 of the center-inversives is also an ellipse (blue), concentric, axis-aligned, and homothetic to the former at ratio $1/\delta$. App

and concentric with the billiard and similar to the caustic (rotated by $\pi/2$). Thus, the locus of X_3^{\odot} must be an ellipse concentric, axis-aligned, and homothetic to that one, with homothety ratio $1/\delta$.

Observation 6. Over X_k , k = 1...1000, only X_3 sweeps a conic locus over the center-inversive family.

6. Videos

Animations illustrating some focus-inversive phenomena are listed on Table 1.

id	Title	${\bf youtu.be}/{<}{>}$
01	N=5 invariants	wkstGKq5jOo
02a	N=3 circumbilliard I	LOJK5izTctI
02b	N=3 circumbilliard II	Y-j5eXqKGQE
03	N=3 invariant area product	0L2uMk2xyKk
04	N=5 invariant area product	bTkbdEPNUOY
05	N=3 equal-area pedals	0L2uMk2xyKk
06a	N=3 circular loci I	OAD2hpCRgCI
06b	N=3 circular loci II	tKB-50zW8F4
06c	N=3 circular loci III	srjm23nQbMc

Table 1. Videos of some focus-inversive phenomena. The last column is clickable and provides the YouTube code.

ACKNOWLEDGMENTS

We would like to thank Arseniy Akopyan, Peter Moses, and Pedro Roitman for useful insights.

The second author is fellow of CNPq and coordinator of Project PRONEX/CNPq/ FAPEG 2017 10 26 7000 508.

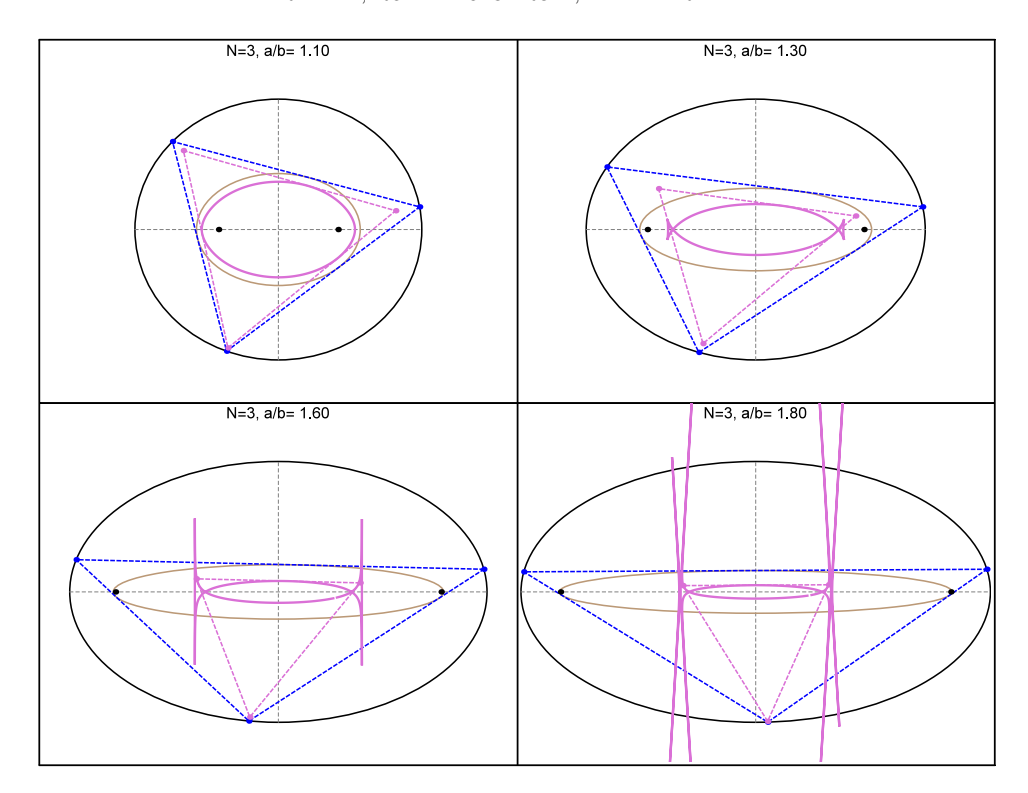


Figure 10. Non-conic caustic (pink) to the center-inversive family (dashed pink). As a/b increases it transitions from (i) a regular-convex curve, to (ii) one with two self-intersections and four cusps, to (iii) a non-compact, self-intersected curve. App1, App2

APPENDIX A. REVIEW: ELLIPTIC BILLIARD

Joachimsthal's Integral expresses that every trajectory segment is tangent to a confocal caustic [20]. Equivalently, a positive quantity J remains invariant at every bounce point $P_i = (x_i, y_i)$:

$$J = \frac{1}{2} \nabla f_i \cdot \hat{v} = \frac{1}{2} |\nabla f_i| \cos \alpha$$

where \hat{v} is the unit incoming (or outgoing) velocity vector, and:

$$\nabla f_i = 2\left(\frac{x_i}{a^2}, \frac{y_i}{b^2}\right).$$

Hellmuth Stachel contributed [19] an elegant expression for Joahmisthal's constant J in terms of EB semiaxes a, b and the major semiaxes a'' of the caustic:

$$J = \frac{\sqrt{a^2 - a''^2}}{ab}$$

The signed area of a polygon is given by the following sum of cross-products [11]:

$$A = \frac{1}{2} \sum_{i=1}^{N} (P_{i+1} - P_i) \times (P_i - P_{i+1})$$

Let $d_{j,i}$ be the distance $|P_i - f_j|$. The inversion $P_{j,i}^{\dagger}$ of vertex P_i with respect to a circle of radius ρ centered on f_j is given by:

$$P_{j,i}^{\dagger} = f_j + \left(\frac{\rho}{d_{j,i}}\right)^2 (P_i - f_j)$$

N=3 case. For N=3 the following explicit expressions for J and L have been derived [8]:

(2)
$$J = \frac{\sqrt{2\delta - a^2 - b^2}}{c^2}$$
$$L = 2(\delta + a^2 + b^2)J$$

When a = b, $J = \sqrt{3}/2$ and when $a/b \rightarrow \infty$, $J \rightarrow 0$.

APPENDIX B. VERTICES & CAUSTICS N=3

Let $P_i = (x_i, y_i)/q_i$, i = 1, 2, 3, denote the 3-periodic vertices, given by [5]:

$$\begin{split} q_1 &= 1 \\ x_2 &= -b^4 \left(\left(a^2 + b^2 \right) k_1 - a^2 \right) x_1^3 - 2 \, a^4 b^2 k_2 x_1^2 y_1 \\ &+ a^4 \left(\left(a^2 - 3 \, b^2 \right) k_1 + b^2 \right) x_1 \, y_1^2 - 2 a^6 k_2 y_1^3 \\ y_2 &= 2 b^6 k_2 x_1^3 + b^4 \left(\left(b^2 - 3 \, a^2 \right) k_1 + a^2 \right) x_1^2 y_1 \\ &+ 2 \, a^2 b^4 k_2 x_1 y_1^2 - a^4 \left(\left(a^2 + b^2 \right) k_1 - b^2 \right) y_1^3 \\ q_2 &= b^4 \left(a^2 - c^2 k_1 \right) x_1^2 + a^4 \left(b^2 + c^2 k_1 \right) y_1^2 - 2 \, a^2 b^2 c^2 k_2 x_1 \, y_1 \\ x_3 &= b^4 \left(a^2 - \left(b^2 + a^2 \right) \right) k_1 x_1^3 + 2 \, a^4 b^2 k_2 x_1^2 y_1 \\ &+ a^4 \left(k_1 \left(a^2 - 3 \, b^2 \right) + b^2 \right) x_1 \, y_1^2 + 2 \, a^6 k_2 y_1^3 \\ y_3 &= -2 \, b^6 k_2 x_1^3 + b^4 \left(a^2 + \left(b^2 - 3 \, a^2 \right) k_1 \right) x_1^2 y_1 \\ &- 2 \, a^2 b^4 k_2 x_1 y_1^2 + a^4 \left(b^2 - \left(b^2 + a^2 \right) k_1 \right) \, y_1^3, \\ q_3 &= b^4 \left(a^2 - c^2 k_1 \right) x_1^2 + a^4 \left(b^2 + c^2 k_1 \right) y_1^2 + 2 \, a^2 b^2 c^2 k_2 \, x_1 \, y_1. \end{split}$$

where:

$$k_1 = \frac{d_1^2 \delta_1^2}{d_2} = \cos^2 \alpha,$$

$$k_2 = \frac{\delta_1 d_1^2}{d_2} \sqrt{d_2 - d_1^4 \delta_1^2} = \sin \alpha \cos \alpha$$

$$c^2 = a^2 - b^2, \quad d_1 = (a \, b/c)^2, \quad d_2 = b^4 x_1^2 + a^4 y_1^2$$

$$\delta = \sqrt{a^4 + b^4 - a^2 b^2}, \quad \delta_1 = \sqrt{2\delta - a^2 - b^2}$$

where α , though not used here, is the angle of segment P_1P_2 (and P_1P_3) with respect to the normal at P_1 .

The caustic is the ellipse:

$$\frac{x^2}{a''^2} + \frac{y^2}{b''^2} - 1 = 0, \quad a'' = \frac{a(\delta - b^2)}{a^2 - b^2}, \quad b'' = \frac{b(a^2 - \delta)}{a^2 - b^2}$$

APPENDIX C. TABLE OF SYMBOLS

symbol	meaning	
O, N	center of billiard and vertex count	
L, J	perimeter and Joachimsthal's constant	
a, b	billiard major, minor semi-axes	
$a^{\prime\prime},b^{\prime\prime}$	caustic major, minor semi-axes	
f_1, f_2	foci	
P_i, θ_i	N-periodic vertices and angle	
$d_{j,i}$	distance $ P_i - f_j $	
A	N-periodic area	
ρ	radius of the inversion circle	
$P_{i,i}^{\dagger}$	vertices of the inversive polygon wrt f_j	
$L_i^{\dagger}, A_i^{\dagger}$	perimeter, area of inversive polygon wrt f_i	
$\theta_{j,i}^{\dagger}$	ith angle of inversive polygon wrt f_j	

Table 2. Symbols used in the invariants. Note $i \in [1, N]$ and j = 1, 2.

References

- [1] Akopyan, A. (2012). Conjugation of lines with respect to a triangle. *Journal of Classical Geometry*, 1: 23-31. users.mccme.ru/akopyan/papers/conjugation_en.pdf.
- [2] Bialy, M., Tabachnikov, S. (2020). Dan Reznik's identities and more. Eur. J. Math. doi.org/10.1007/s40879-020-00428-7.
- [3] Ferréol, R. (2020). Booth's curve. Mathcurve Portal. https://mathcurve.com/courbes2d.gb/booth/booth.shtml.
- [4] Ferréol, R. (2020). Pascal's limaçon. Mathcurve Portal. https://mathcurve.com/courbes2d.gb/limacon/limacon.shtml.
- [5] Garcia, R. (2019). Elliptic billiards and ellipses associated to the 3-periodic orbits. American Mathematical Monthly, 126(06): 491–504.
- [6] Garcia, R., Reznik, D. (2020). Invariants of self-intersected and inversive n-periodics in the elliptic billiard.
- [7] Garcia, R., Reznik, D., Koiller, J. (2020). Loci of 3-periodics in an elliptic billiard: why so many ellipses? Submitted.
- [8] Garcia, R., Reznik, D., Koiller, J. (2020). New properties of triangular orbits in elliptic billiards. *Amer. Math. Monthly*, to appear.
- [9] Kaloshin, V., Sorrentino, A. (2018). On the integrability of Birkhoff billiards. Phil. Trans. R. Soc., A(376).
- [10] Kimberling, C. (2019). Encyclopedia of triangle centers. faculty.evansville.edu/ck6/encyclopedia/ETC.html.
- [11] Preparata, F., Shamos, M. (1988). Computational Geometry An Introduction. Springer-Verlag, 2nd ed.
- [12] Reznik, D., Garcia, R. (2021). Circuminvariants of 3-periodics in the elliptic billiard. Intl. J. Geometry, 10(1): 31–57.
- [13] Reznik, D., Garcia, R., Koiller, J. (2020). The ballet of triangle centers on the elliptic billiard. Journal for Geometry and Graphics, 24(1): 079–101.
- [14] Reznik, D., Garcia, R., Koiller, J. (2020). Can the elliptic billiard still surprise us? Math Intelligencer, 42: 6-17. rdcu.be/b2cg1.
- [15] Reznik, D., Garcia, R., Koiller, J. (2021). Eighty new invariants of n-periodics in the elliptic billiard. Arnold Math. J. ArXiv:2004.12497.
- [16] Roitman, P. (2020). Sum of focus-to-inversive-vertex distances is conserved. Private Communication.

- [17] Romaskevich, O. (2014). On the incenters of triangular orbits on elliptic billiards. Enseign. Math., 60(3-4): 247–255. arxiv.org/pdf/1304.7588.pdf.
- [18] Schwartz, R., Tabachnikov, S. (2016). Centers of mass of Poncelet polygons, 200 years after. Math. Intelligencer, 38(2): 29–34. bit.ly/3kLetNU.
- [19] Stachel, H. (2020). Private Communication.
- [20] Tabachnikov, S. (2005). Geometry and Billiards, vol. 30 of Student Mathematical Library. Providence, RI: American Mathematical Society. bit.ly/2RV04CK.
- [21] Weisstein, E. (2019). Mathworld. mathworld.wolfram.com.